The roles of microstructure and mechanics in intergranular stress corrosion cracking

The roles of microstructure and mechanics in intergranular stress corrosion cracking

A P Jivkov, N P C Stevens and T J Marrow
School of Materials, The University of Manchester, Manchester M60 1QD, UK.

Abstract

Previous work on the prediction of intergranular stress corrosion cracking resistance in grain boundary engineered microstructures has used two dimensional percolation models, in which the grain boundaries are assumed to be either resistant or susceptible to cracking, depending on the grain boundary character. One limitation of such models is that they do not necessarily account for the mechanical crack driving force. Further, they cannot capture experimentally observed phenomena such as the formation of isolated ductile bridging ligaments by resistant boundaries. These arise due to the three-dimensional character of crack propagation. A new mechanical crack propagation model is presented which, via finite element solutions, addresses these limitations. The model is based on a regular discrete representation of the material's microstructure and is applicable to both 2D and 3D behaviour. Results are reported for 2D-hexagonal microstructures, and are compared with percolation models. The results demonstrate the influence of stress on crack path, as well as the influence of the rupture strain of susceptible boundaries on crack behaviour. Further, the effect of crack bridging, which arises from ductile resistant boundaries is studied.

Keywords: Intergranular stress corrosion; Microstructure; Mechanics; Crack bridging; Finite elements; Monte Carlo simulations.

1 Introduction

It has been increasingly realised during the last two decades, that the grain size is not the only meso-scale factor influencing the strength of polycrystalline materials. Two other factors have been brought to wider attention. The first is the

grain boundary character distribution (GBCD) which describes the fractions of boundaries with different energies, with “special” or low-energy boundaries having higher resistance to intergranular deterioration mechanisms and “random” or high-energy boundaries having lower resistance. The second factor is the topological connectivity of “random” boundaries. In connection to these findings, the concept of grain boundary engineering has been introduced by Watanabe [1]. The primary purpose of grain boundary engineering has been to improve the bulk mechanical properties of polycrystalline materials by increasing the number of “special” boundaries. Together with applications to enhance general fracture toughness [2-4], it has been shown that the “special” grain boundaries can be much less susceptible to intergranular corrosion and stress corrosion cracking (SCC) [5-7]. Since the introduction of grain boundary engineering, characterisation of grain boundary networks has been an important topic in grain boundary engineering research [8-11]. Predictive stress corrosion cracking models aim to determine the probability of crack arrest and distribution of arrested crack lengths for given grain boundary network characteristics. Previously proposed models [12-16] used a percolation-type process to determine the probable extent of crack growth. These are binary models, i.e. a grain boundary is assumed to be either entirely resistant or entirely susceptible to SCC. In the early models [12, 13], the probability of crack advance at a junction is based on the GBCD and orientation of the grain boundary with respect to the applied stress. Later models [14-16], additionally account for the network connectivity via the distribution of triple junctions. All these models, however, cannot describe the effects of the applied stress magnitude or stress redistribution during crack evolution. Hence, they stand close to a pure geometrical percolation model, giving the critical share of “random” boundaries above which a continuous crack path across a given microstructure is always possible. For the most widely used two dimensional hexagonal cell structure [12,13,15], the critical share of resistant boundaries (i.e. the percolation threshold) is found to be around 0.65, while for the space-filling tetrakaidecahedral structure in three dimensions [1,5], the threshold is around 0.23 (see e.g. [14]). Previous 2D models also cannot account for the experimentally observed crack bridging behaviour. Bridging is created by the yielding of ductile ligaments, formed by resistant boundaries left behind the advancing crack front in the real 3D geometry. A recently proposed analytical model [17], has attempted to take into account the effects of crack bridging on the local crack tip stress intensity factor, thus mimicking 3D crack behaviour.

The objective of the present work is to combine the structural development of a percolation model with actual finite element calculations of the stress after each change in geometry due to crack advance. This allows for a more accurate simulation of crack evolution, as the probability of crack advance depends upon the actual mechanical conditions at the crack tip. This is affected by the crack propagation history, i.e. the effects of crack branching, crack bridging and redistribution of the initial stress state. The work utilises a regular 2D hexagonal cell structure. Grain boundaries are assumed to belong to either of the two classes – susceptible or resistant to stress corrosion. All boundaries belonging to

one class are assigned identical mechanical properties. Susceptible boundaries are assumed to fail at crack opening displacements of the order of several nanometers. This represents a local crack propagation criterion requiring a small level of crack tip strain, suggested by experimental observations of intergranular stress corrosion [18]. Resistant boundaries are assumed to deform in a ductile manner, as demonstrated by in-situ high resolution tomographic and fractographic observations of intergranular stress corrosion cracking [19]. The particular physical mechanism of cracking and hence the time-scale of crack propagation process are not involved in this work.

2 Model description

A possible approach to modelling an assembly of hexagonal cells (grains) in a finite element environment could be based on continuum mechanics. Each cell could be tessellated into continuum elements, e.g. triangles, and connected to the neighbouring cells with interface elements representing the boundary between the two grains. Such a direct strategy would require significant computational resources for the simulations when the size of the assembly increases. A simpler structural model of the grain network is proposed and used in this work. In this model, each cell is represented by a geometrical point and its connections to the neighbouring cells are represented by linear structural members. The scheme is illustrated in Fig. 1, where a portion of a plane hexagonal mesh and its corresponding structure are shown. The finite element model consists of nodes in the centres of the grains, and plane beam elements as structural members.

Let D denote the diameter of a hexagonal cell. With respect to a fixed coordinate system (X_1, X_2), the assembly of grains studied in this work fills the rectangular region $\{-50D \le X_1 \le 50D,\ 0 \le X_2 \le 50D\}$. This region contains 7740 grains, which form 22850 internal grain boundaries, modelled by 7740 nodes and 22850 beam elements in the finite element model.

An initial crack, extending along three grain boundaries, is introduced from the surface point at the origin of the two axis in the coordinate system and running in towards the centre of the element assembly. This is schematically shown with a

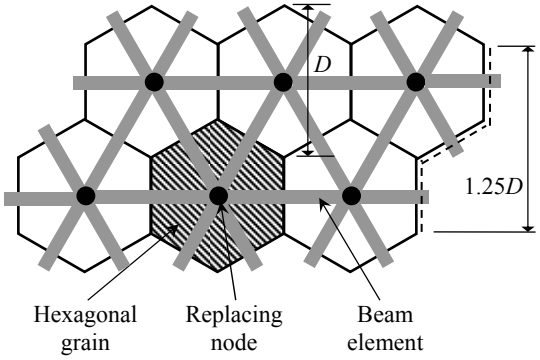

Figure 1: Illustration of the discrete model of hexagonal microstructure

dashed line on the right of Fig. 1, where the length of the pre-crack is also given as 1.25*D*. The geometry of the crack and the boundary conditions define an initial stress intensity factor approximately as

$$K_I \approx 1.1215\,\sigma_\infty \sqrt{\pi (1.25D)} \tag{1}$$

where σ_∞ is the remotely applied stress and the stress pre-factor accounts for the edge crack geometry (see e.g. [20]).

An important question in the proposed structural model of a polycrystalline solid is the choice of geometrical and mechanical properties of structural members, so that the model represents properly the assembly behaviour. In this work, the cross section of the beam elements is chosen in such a way that their elastic properties (Young's modulus, E, and Poisson's ratio, ν) coincide with the bulk metal properties, namely E = 200 GPa and ν = 0.3, while at the same time the assembly overall deformation under considered boundary conditions is the same as the deformation of a continuous solid of the same geometry.

Two groups of grain boundaries in an assembly are considered: those susceptible and those resistant to corrosion. The susceptible boundaries are assumed to fail at a small crack opening displacement when encountered by the propagating crack. The strain at failure, ε_f, is the property that determines the mechanical behaviour of these susceptible boundaries. The resistant boundaries are assumed to be elastic-plastic with linear isotropic hardening described by the following parameters: yield stress σ_y = 200 MPa at yield strain $\varepsilon_y = 10^{-3}$; ultimate strength σ_u = 400 MPa at ultimate strain ε_u = 0.1. The constitutive boundary properties are illustrated in Fig. 2. In summary, all boundaries have identical elastic properties, but the susceptible ones fail completely if the prescribed critical strain is reached, while the resistant ones yield. For a given fraction of susceptible boundaries a random distribution of these boundaries are applied to the structural elements.

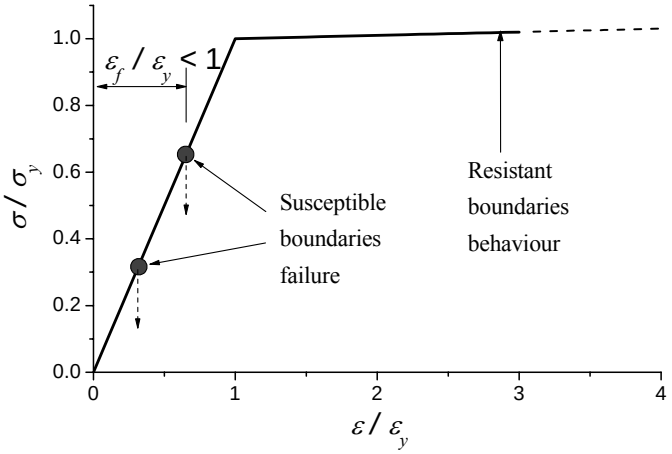

Figure 2: Schematic for constitutive behaviour of boundaries

The load is symmetric and applied via prescribed displacements: $u_1 = -0.025D$ along the boundary $\{X_1 = -50D,\ 0 \le X_2 \le 50D\}$ and $u_1 = 0.025D$ along the boundary $\{X_1 = 50D,\ 0 \le X_2 \le 50D\}$. Displacements $u_2 = 0$ are prescribed along the boundary $\{-50D \le X_1 \le 50D,\ X_2 = 50D\}$, while zero stresses are prescribed for all other boundary conditions. This introduces a homogeneous strain in the assembly $\varepsilon_\infty = 5\text{x}10^{-4}$, equivalent to a homogeneous stress $\sigma_\infty \approx 0.5\sigma_y$.
Two types of crack advance behaviour have been considered: Type A, where no bridging by ductile ligaments (resistant boundaries) is allowed and the crack arrests when it cannot rupture any boundary adjacent to the crack surface; and Type B, where the crack is effectively allowed to by-pass resistant boundaries and propagate further if a susceptible boundary from the first subsurface layer adjacent to the arrested crack tip could be ruptured, i.e. cracks which would arrest in Type A may be able to propagate further in type B, leaving a ductile ligament behind the crack tip. In Type B, a reduced rupture strain, ε_r, is used for the failure criterion of subsurface boundaries. This accounts for the propagation of the crack in three dimensions around the resistant boundary, which would locally raise the strain at the subsurface boundary in the 2D model. In order to define the reduced rupture strain used for Type B propagation, it is important to estimate the strain at the midpoints (which are also the integration points) of the beam elements in the vicinity of the crack tip. This can be approximately done by imagining a straight crack in a homogeneous body under plane strain conditions with the same X_2-extension as the intergranular crack. Fig. 3 illustrates the argument for the two possible cases of the imaginary crack position, denoted by 1 and 2 respectively (see also Fig. 1). For this purpose, it is useful to express the tangential strains in polar coordinates (e.g. [20]):

$$\varepsilon_t = \frac{1-\nu^2}{E}\frac{K_I}{\sqrt{2\pi r}}\left[\cos^3\frac{\theta}{2} - \frac{\nu}{1-\nu}\cos\frac{\theta}{2}\left(1+\sin^2\frac{\theta}{2}\right)\right] \qquad (2)$$

where K_I is the current stress intensity, r and θ are the polar coordinates of the point in question with respect to a polar coordinate system centred at the tip and having a zero axis parallel to crack propagation direction.

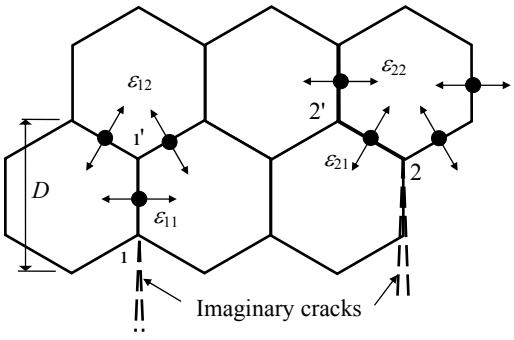

Figure 3: Estimation of grain boundary strains.

For the closest boundary in case 1, the tensile strain in the corresponding beam element is approximately equal to ε_{11}, which could be calculated from Eqn (2) with $r = D / 4$ and $\theta = 0$. For the closest boundaries in case 2, the tensile strain in the corresponding beam element is approximately equal to ε_{21}, calculated from Eqn (2) for $r = D / 8$ and $\theta = \pi / 3$. From (1) and (2), for example, the initially introduced crack in Fig. 1 causes a tensile strain in the two adjacent inclined beam elements approximately equal to $0.5\varepsilon_{\infty}$. This is a conservative estimate, but offers an indication of the susceptible boundaries' failure strain. The use of a much larger ε_f would make crack advance impossible.

In a similar but more elaborate way, the strains in the subsurface boundaries, ε_{12}, and ε_{22}, could be calculated. In Type B crack advance, if the boundaries adjacent to the tip are resistant, it is assumed that the crack bypasses them, mimicking 3D behaviour, and arrives at point 1' or 2' in Fig. 3. Then the real strain in the subsurface boundaries for case 1 would be approximately ε_{21}, while the real strain in the subsurface boundaries for case 2 would be approximately ε_{11} (neglecting the small change in stress intensity due to crack advance). In order to simulate this situation in the 2D settings, the failure strain of the subsurface boundaries should be reduced by a factor $\alpha_1 = \varepsilon_{12} / \varepsilon_{21} \approx 1.0$ for position 1 and by a factor $\alpha_2 = \varepsilon_{22} / \varepsilon_{11} \approx 0.77$ for position 2, respectively. To simplify the calculations a reduction factor $\alpha = (\alpha_1 + \alpha_2) / 2$ is chosen for all subsurface boundaries, so that $\varepsilon_r = \alpha \varepsilon_f$.

3 Crack advance simulations

The problem of crack propagation is split into evolution and equilibrium parts and these are handled by two separate software components. The first component, an in-house made program, is used for preparation of initial geometry, boundary conditions and a randomised distribution of the structural members' properties. The boundary value problem thus formulated is solved by the commercial finite element program ABAQUS [21]. The solution delivered by ABAQUS is used by the in-house program, which traverses all elements with nodes belonging to the crack surface to localise the most strained element. The decision on whether the crack will propagate is based on the following rules:

(1) If the most strained element is susceptible and the tensile strain $\varepsilon > \varepsilon_f$, then the element is removed from the structure and the simulation continues.

(2) If the most strained element is resistant and yields, then:

- (2a) For series A the crack is assumed arrested and the simulation terminates.
- (2b) For series B the elements in its immediate vicinity under the crack surface are considered; if the most strained of them has a tensile strain $\varepsilon > \varepsilon_r$, then this element is removed from the structure and the simulation continues. If there is no such element the crack is arrested and the simulation terminates.

In case of crack continuation, at most one structural member is allowed to fail and is then removed from the structure. This changed geometry constitutes a new

boundary value problem, which is formulated by the in-house program and solved by ABAQUS. The process is repeated either until crack arrest or until the crack X_2-extension reaches a prescribed limit of half the assembly, $L = 25D$. It is assumed that a crack reaching the limit L fractures the assembly.

4 Results and discussion

4.1 2D simulations – Type A

For 2D simulations without bridging, attention was focussed on the differences between strain-directed crack propagation in comparison with a pure percolation model. Simulations were performed for a series of susceptible boundary fractions, *f = (Number of susceptible boundaries / Total number of boundaries)*, ranging from 0.1 to 0.9. For each *f*, a Monte Carlo type of solution was utilised,

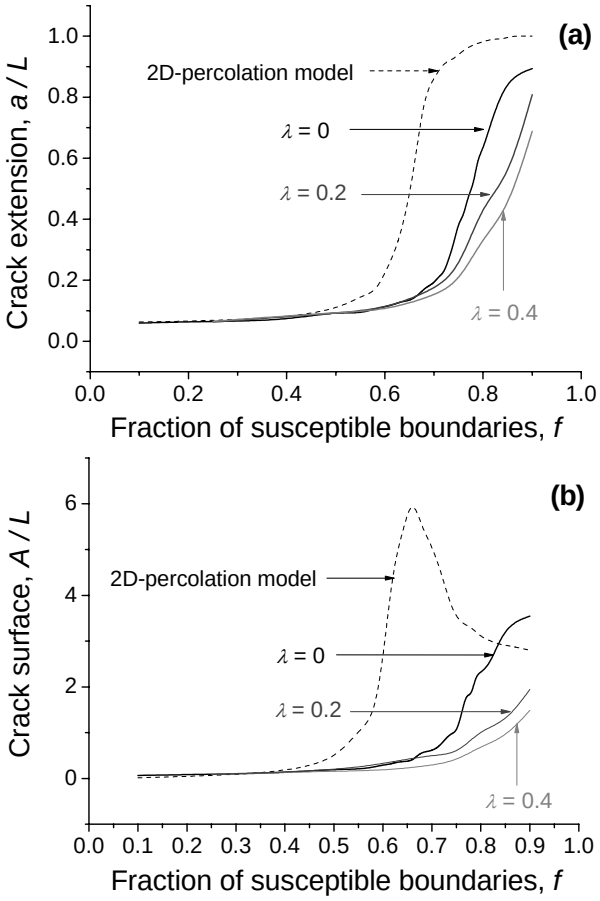

Figure 4: Expected crack extension (a) and expected crack area (b) as a function of susceptible boundaries fraction for Type A advance

with 30 different random distributions of susceptible boundaries. Each of these determined a separate crack evolution problem which was solved as described in the previous section. For comparison, pure percolation simulations for the same fractions and distributions were also performed. The parameters monitored for each finite element evolution problem or crack percolation problem were the final crack extension (the crack projection on X_2-axis) and the total crack area (given by total number of ruptured boundaries, i.e. including all crack branches). For each f, the average of crack extensions and the average of crack areas from the 30 random distribution solutions was found, and is taken to represent the expected crack extension, a, and crack area, A, for this particular fraction of susceptible boundaries. Results for the crack extensions and crack areas are presented in Fig. 4a and Fig. 4b, respectively, for the pure percolation model and for the finite element model with three choices of susceptible boundary rupture strain, given by $\lambda = \varepsilon_f / \varepsilon_\infty = 0$; 0.2; 0.4. The results are normalised with respect to the limiting crack length, L. Note that the simulations with $\lambda = 0$ correspond to the early percolation models based on GBCD and favourable orientation of grain boundary with respect to applied stress [12,13]. It is evident for the case $\lambda = 0$ that the role of mechanical strain is to direct the crack growth by decreasing crack branching. There is also an increase in the fraction of susceptible boundaries needed to develop a crack of given extension compared to the pure percolation model. This case is effectively a limiting solution for infinite applied stress. For finite values of remotely applied stress, any increase of the strength of susceptible boundaries increases the fracture resistance of the assembly, by increasing the fraction needed for given crack extension at a given applied stress.

4.2 Quasi 3D simulations – Type B

The model with bridging allows more realistic simulations of crack propagation. It is expected that the model should show intermediate behaviour between pure 2D and 3D percolation behaviour. Therefore, full 3D percolation simulations using assemblies of tetrakaidecahedrons were also performed for comparison. A tetrakaidecahedron is a body bounded by six squares and eight regular hexagons, having cubic and octahedral symmetry. As this structure cannot be directly represented in 2D, the 3D percolation results may be used as a qualitative illustration of the expected behaviour of a system in which fully three dimensional bridging is possible. As in the previous 2D model, finite element simulations were performed for f ranging from 0.1 to 0.9, and for each fraction 30 different random distributions of susceptible boundaries were considered. The results of all simulations are summarised in Fig. 5, where the same notations and scaling conventions as in Fig. 4 are used. The results show that the bridging indeed gives behaviour closer to the 3D percolation, with a major controlling parameter being the failure strain of the susceptible boundaries, ε_f, for given applied strain, ε_∞. Such a parametric study could be used to find an average value for ε_f from experimental results for crack length distributions, potentially turning the 2D-bridging model into predictive tool. The application of a true 3D tetrakaidecahedral model along the same lines as in this work is currently limited

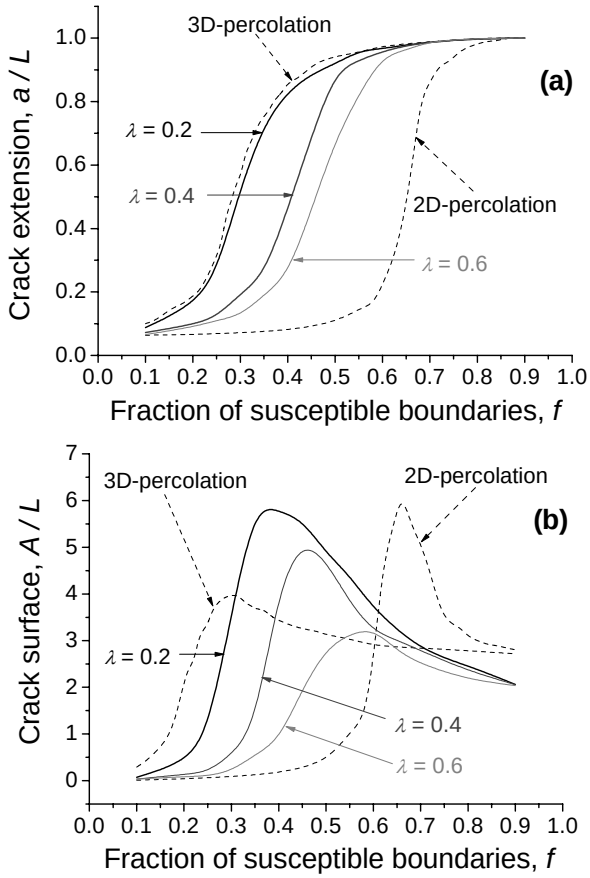

Figure 5: Expected crack extension (a) and expected crack area (b) as a function of susceptible boundaries fraction in Type B advance

by the computational resources available. A small scale model could be useful for tuning the 2D-bridging model with information on crack bridging behaviour. The 2D model could then be used on larger grain assemblies to investigate crack behaviour in stress gradients, for example.

5 Conclusions

The proposed discrete structural model has the potential to simulate intergranular crack propagation in a realistic manner by including the phenomenon of crack bridging by ductile ligaments. It is applicable to sufficiently large grain aggregates in two dimensions to represent an entire test specimen. It accounts for the effects of external load magnitude and failure properties of susceptible boundaries. These effects are demonstrated in Fig. 4 and Fig. 5 in comparison to the results of previous percolation models. Parametric studies of the type

presented in the work related to experimental observations of intergranular stress corrosion crack extensions and distributions are expected to tune the model parameters.

Acknowledgments

The authors gratefully acknowledge the support of this project by Rolls Royce plc.

References

[1] Watanabe T, *Res Mechanica* 11 (1): 47-84, 1984.
[2] Lim LC, Watanabe T, *Acta Metall. Mater.* 38 (12): 2507-2516, 1990.
[3] Watanabe T, *Mater. Sci. Engng.* A176 (1-2): 39-49, 1994.
[4] Watanabe T, Tsurekawa S, *Acta Mater.* 47 (15-16): 4171-4185, 1999.
[5] Lin P, Palumbo G, Erb U, Aust KT, *Scripta Metall. Mater.* 33 (9): 1387-1392, 1995.
[6] Lehockey EM, Palumbo G, Lin P, Brennenstuhl AM, *Scripta Mater.* 36 (10): 1211-1218, 1997.
[7] Gertsman VY, Bruemmer SM, *Acta Mater.* 49 (9): 1589-1598, 2001.
[8] Garbacz A, Grabski MW, *Acta Metall. Mater.* 41 (2): 469-473, 1993.
[9] Gertsman VY, Tangri K, Valiev RZ, *Acta Metall. Mater.* 42 (6): 1785-1804, 1994.
[10] Randle V, *Acta Metall. Mater.* 42 (6): 1769-1784, 1994.
[11] Davies P, Randle V, Watkins G, Davies H, *J. Mater. Sci.* 37: 4203-4209, 2002.
[12] Palumbo G, King PJ, Aust KT, Erb U, Lichtenberger PC, *Scripta Metall. Mater.* 25 (8): 1775-1780, 1991.
[13] Aust KT, Erb U, Palumbo G, *Mater. Sci. Engng.* A176 (1-2): 329-334, 1994.
[14] Gertsman VY, Janecek M, Tangri K, *Acta Mater.* 44 (7): 2869-2882, 1996.
[15] Gertsman VY, Tangri K, *Acta Mater.* 45 (10): 4107-4116, 1997.
[16] Lehockey EM, Brennenstuhl AM, Thompson I, *Corr. Sci.* 46 (10): 2383-2404, 2004.
[17] Engelberg DL, Marrow TJ, Newman RC, Babout L, In: *Proc. 2nd Int. Conf. Environment-induced Cracking of Metals*, 2004 (in press).
[18] Thomas LE, Bruemmer SM, *Corrosion* 56: 572-587, 2000.
[19] Marrow TJ, Babout L, Connolly BJ, Engelberg D, Johnson G, Buffiere J-Y, Withers PJ, Newman RC, In: *Proc. 2nd Int. Conf. Environment-induced Cracking of Metals*, 2004 (in press).
[20] Tada, H., Paris, P.C. & Irwin, G.R., *The stress analysis of cracks handbook*, 3d Ed. ASME Pres: New York, 2000.
[21] ABAQUS User's Manual, Version 6.4, Abaqus Inc., 2004.